Radar time budget optimization subject to angle accuracy constraint via cognitive approach

Michał Meller[*]

[*]PIT-RADWAR S.A.
ul. Poligonowa 30, 04-051 Warsaw, POLAND
Gdańsk University of Technology, Department of Automatic Control
Faculty of Electronics, Telecommunications and Computer Science
ul. Narutowicza 11/12, 80-233 Gdańsk, POLAND
email: michal.meller@eti.pg.gda.pl

Abstract: *The problem of minimizing dwell time in multifunction phased array radar is considered. Target of interest is assumed to fluctuate according to a generalization of Swerling family and the parameters of fluctuation model are assumed to be known. The a'priori position of the target is uncertain. Optimization, whose variables include pulse count and array transmit beampattern, is carried out subject to achieving a desired accuracy of angular coordinate estimates.*

1. Introduction

An important capability of multifunction is their ability to perform multiple tasks simultaneously. This is done by rapid interleaving of dwells corresponding to different functions, or modes. Typical examples of modes include, among others, volume search, long range horizon scan and tracking of detected targets.

Due to different requirements of each mode, design of multifunction radars involves many unavoidable conflicts, starting from as fundamental ones as choice of operating band [1]. One of major difficulties encountered in actual operation is that of scheduling, or radar time budget management. Since execution of each function requires time, there is only a finite amount of tasks that the radar can handle in a given amount of time. In congested environments this limitation may become a critical bottleneck.

Compared to legacy systems, modern software defined radars offer much more flexibility in selecting waveform parameters. For instance, pulse modulation, width, repetition frequency, burst length or aperture illumination can be varied with great freedom. This opens new opportunities for radar scheduler – the waveform can be tailored to *actual* operation needs for each mode and target individually. Due dependence of most performance metrics on a product of signal to noise ratio and integration time, and strong dependence of signal to noise ratio on a distance to the target, considerable savings of time can be made in most but a few rare cases.
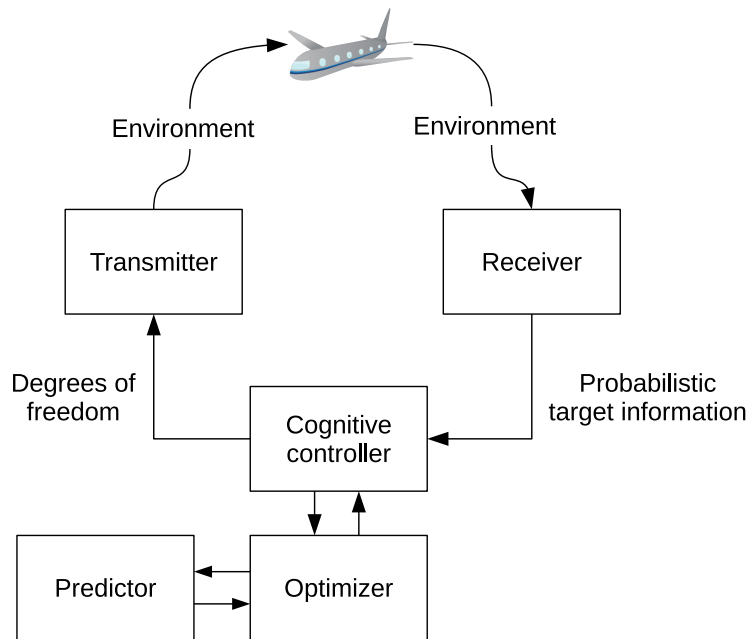
Figure 1: Simplified block diagram of cognitive radar.

The problem of radar resource management can be handled rigorously within cognitive radar framework (Fig. 1). In this approach the cognitive controller provides strong feedback between the receiver and the transmitter. What differs cognitive radar from current state of the art approaches, which often rely on heuristic decision rules, is that to make its decisions the cognitive controller works out predictions of applicable figures of merit and performs optimization in the space of available transmit degrees of freedom [2]. This means that resulting actions are close to the optimal ones.

Although cognitive radar was introduced as a mean to increase accuracy in demanding tracking applications [3] or to improve detection [4], it was soon realized that perhaps one of the most important benefits offered by cognition is that it allows one to use radar resources more effectively – achieving ultimate performance, in the sense of e.g. minimizing mean squared tracking errors, is usually not as desirable as achieving just the *right* amount of performance and being able to handle more tasks.

In this paper cognitive radar framework is used to minimize observation time of target under tracking. Since reduction of observation time adversely affects almost all performance metrics, optimization must be carried out subject to some constraints. Typical constraints could include probability of detection, clutter visibility or accuracy of target position estimation. Here we choose ta constrain the accuracy of target angular coordinate estimation. We choose to do so, because in many scenarios achieving desired accuracy of angular estimates requires such a value of SNR which automatically fulfills requirement on probability of detection and range estimation accuracy. Clutter visibility is not considered due to space constraints.

The text is organized as follows. Section 2 presents problem formulation. Prediction of angle ac-

2

curacy is carried out in section 3. Sections 4 and 5 discuss optimization and simulation example, respectively. Section 6 concludes.

2. Problem formulation

Suppose that the radar is to transmit a pulse burst of n_P pulses, where n_P is to be found by cognitive controller. Echo signal received during the n-th pulse interval, $n = 1, 2, \ldots, n_P$, is modeled as

$$\boldsymbol{y}_n = Fre^{j\phi_n} B_T(\boldsymbol{w}_T, \alpha) \boldsymbol{a}(\alpha) + \boldsymbol{v}_n \; , \tag{1}$$

where F is a coefficient which models signal decay during two-way propagation and other losses, $r^2 = \sigma$ denotes radar cross section (RCS) of the target, ϕ_n is echo phase during n-th pulse interval, α is target angle and $\boldsymbol{a}(\alpha)$ is array steering vector at target angle. The quantity

$$B_T(\boldsymbol{w}_T, \alpha) = \boldsymbol{w}_T^{\mathrm{H}} \boldsymbol{a}(\alpha)$$

is transmit beampattern at the target when the transmit beam is formed using complex array weights given by vector $\boldsymbol{w}_T$. Finally, $\boldsymbol{v}_n$ denotes measurement noise, assumed to form a zero mean i.i.d. complex circular Gaussian white noise with covariance matrix $\sigma_v^2 \boldsymbol{I}$, where $\boldsymbol{I}$ denotes eye matrix with size matching the sizes of $\boldsymbol{v}_n$ and $\boldsymbol{y}_n$.

Target angle α is assumed to be a Gaussian random variable, $\alpha \sim \mathcal{N}(\alpha_0, \sigma_\alpha^2)$. In the target tracking scenario this would be a'priori (predictive) distribution obtained from radar tracker.

Target RCS σ is γ-distributed random variable with known shape and rate parameters, $\gamma_s > 1$, $\gamma_r > 0$, respectively. Note that γ distribution is a generalization of chi-squared family of Swerling models [5] – Swerling I model is obtained for $\gamma_s = 1$, while Swerling III case requires $\gamma_s = 2$. Values of γ_s between 1 and 2 yield intermediate cases. Furthermore, for any choice of γ_s, γ_r, average target RCS is given by their ratio

$$\sigma_{av} = \mathrm{E}[\sigma] = \frac{\gamma_s}{\gamma_r} \; .$$

Noncoherent and coherent processing case will be considered. The former is readily obtained by assuming that ϕ_n, $n = 1, 2, \ldots, n_P$ forms a i.i.d. sequence of random variables uniformly distributed in $[0, 2\pi)$. The latter will be handled in a slightly less rigorous way which reflects actual processing being done typically.

The cognitive controller goal is to minimize

$$f(n_P, \boldsymbol{w}_T) = n_P + Q(\boldsymbol{w}_T) \; , \tag{2}$$

where $Q(\boldsymbol{w}_T)$ represents the cost of using distribution $\boldsymbol{w}_T$, subject to

$$n_P \in \mathcal{N}_P$$
$$P(\Delta\hat{\alpha}^2) < \Delta\alpha_{\max}^2 \tag{3}$$

3

where $\mathcal{N}_P$ denotes the set of admissible pulse trail lengths, $\Delta\hat{\alpha}$ is angle estimation error

$$\Delta\alpha = \alpha - \hat{\alpha} , \tag{4}$$

of conditional maximum likelihood (ML) angle estimate $\hat{\alpha}$, $P(\Delta\hat{\alpha}^2)$ is predicted mean square error of this estimate and $\Delta\alpha_{\max}^2$ sets the desired level of accuracy.

3. Estimation accuracy prediction

3.1. Noncoherent processing case

Given an unknown deterministic parameter vector

$$\boldsymbol{\theta}_{\mathrm{nc}} = [\alpha \ r \ \phi_1 \ \ldots \ \phi_{n_P}]^{\mathrm{T}} ,$$

which exceeds a certain threshold signal to noise ratio, performance of ML estimator is well predicted by the classical Cramér-Rao lower bound (CRB) [6]

$$\mathrm{E}[\Delta\alpha^2] \geq [\mathbf{FIM}_{\mathrm{nc}}(\boldsymbol{\theta})^{-1}]_{1,1}$$

where

$$\mathbf{FIM}_{\mathrm{nc}}(\boldsymbol{\theta}) = \mathrm{E}_{\boldsymbol{v}_1\ldots\boldsymbol{v}_N}\left[\left(\frac{\partial l}{\partial\boldsymbol{\theta}_{\mathrm{nc}}}\right)\left(\frac{\partial l}{\partial\boldsymbol{\theta}_{\mathrm{nc}}}\right)^{\mathrm{T}}\right]$$

denotes Fisher information matrix and $l(\cdot)$ denotes log-likelihood function of measurements $\boldsymbol{y}_1, \boldsymbol{y}_2, \ldots, \boldsymbol{y}_{n_P}$.

However, in the case considered, all the parameters in $\boldsymbol{\theta}$ are actually random quantities. Due to adopted definition of constraints (3), which measures estimation errors at the output of ML estimator rather than tracker, a Bayesian version of CRB, so called posterior Cramér-Rao lower bound (PCRB), does not apply here as well. This is because PCRB includes prior information, i.e. it would yield optimistic performance estimates.

We will use so called extended Miller-Chang bound (EMCB), defined as [7]

$$\mathrm{EMCB}_{\mathrm{nc}} = \mathrm{E}_{\boldsymbol{\theta}}[[\mathbf{FIM}_{\mathrm{nc}}(\boldsymbol{\theta})^{-1}]_{1,1}] , \tag{5}$$

where $\mathrm{E}_{\boldsymbol{\theta}}[\cdot]$ denotes averaging over all possible values of $\boldsymbol{\theta}$. Note that EMCB can be interpreted as expected value of CRB, so it indeed provides predictions of average ML estimator accuracy.

Due to Gaussian assumptions on measurement noise the matrix $\mathbf{FIM}_{nc}(\boldsymbol{\theta})$ can be found with standard approach [6]. Furthermore, applying the Schur complement technique to get rid of nuisance parameters $r, \phi_1, \ldots, \phi_{n_P}$ one can obtain a closed form solution for $[\mathbf{FIM}_{\mathrm{nc}}(\boldsymbol{\theta})^{-1}]_{1,1}$.

Let

$$S = B_T(\boldsymbol{w}_T, \alpha)\boldsymbol{a}(\alpha)$$

$$T = \frac{\partial B_T(\boldsymbol{w}_T, \alpha)}{\partial \alpha}\boldsymbol{a}(\alpha) + B_T(\boldsymbol{w}_T, \alpha)\frac{\partial \boldsymbol{a}(\alpha)}{\partial \alpha}$$

$$Z_1 = T^{\mathrm{H}}T$$

$$Z_2 = S^{\mathrm{H}}T$$

$$Z_3 = S^{\mathrm{H}}S$$

$$(6)$$

then it can be shown that

$$[\mathbf{FIM}_{\mathrm{nc}}(\boldsymbol{\theta})^{-1}]_{1,1} = \frac{\sigma_v^2}{2F^2 r^2}\left(K_1 - \boldsymbol{K}_2^{\mathrm{T}}\boldsymbol{K}_3^{-1}\boldsymbol{K}_2\right)^{-1} \tag{7}$$

where

$$K_1 = n_P Z_1$$

$$\boldsymbol{K}_2 = \mathrm{Re}\left\{\begin{bmatrix} n_P Z_2 & -jZ_2 & -jZ_2 & \dots & -jZ_2 \end{bmatrix}^{\mathrm{T}}\right\}$$

$$\boldsymbol{K}_3 = \mathrm{diag}\left(n_P Z_3, \ Z_3, \ Z_3, \ \dots, \ Z_3\right) . \tag{8}$$

Further simplifications yield

$$[\mathbf{FIM}_{\mathrm{nc}}(\boldsymbol{\theta})^{-1}]_{1,1} = \frac{\sigma_v^2}{2n_P F^2 r^2}\left(Z_1 - \frac{|Z_2|^2}{Z_3}\right)^{-1}$$

$$= \frac{\sigma_v^2}{2n_P B_T^2(\boldsymbol{w}_T, \alpha)F^2 r^2}\left[\left\|\frac{\partial \boldsymbol{a}(\alpha)}{\partial \alpha}\right\|^2 - \left(\frac{\partial \boldsymbol{a}(\alpha)}{\partial \alpha}\right)^{\mathrm{H}}\frac{\boldsymbol{a}(\alpha)\boldsymbol{a}^{\mathrm{H}}(\alpha)}{\|\boldsymbol{a}(\alpha)\|^2}\frac{\partial \boldsymbol{a}(\alpha)}{\partial \alpha}\right]^{-1}, \tag{9}$$

where $\|\boldsymbol{x}\|^2 = \boldsymbol{x}^{\mathrm{H}}\boldsymbol{x}$.

All that is left to find $\mathrm{EMCB}_{\mathrm{nc}}$ is to perform averaging over r and α. The averaging can be separated into two steps. First, we perform averaging over r. Using the fact that $r^2 = \sigma$ is γ distributed one obtains

$$\mathrm{E}\left[\frac{1}{r^2}\right] = \frac{\gamma_r}{\gamma_s - 1} = \frac{1}{\sigma_{av} - \frac{1}{\gamma_r}} . \tag{10}$$

Second step, i.e. averaging the term

$$G(\boldsymbol{w}_T, \alpha) = \frac{1}{B_T^2(\boldsymbol{w}_T, \alpha)}\left[\left\|\frac{\partial \boldsymbol{a}(\alpha)}{\partial \alpha}\right\|^2 - \left(\frac{\partial \boldsymbol{a}(\alpha)}{\partial \alpha}\right)^{\mathrm{H}}\frac{\boldsymbol{a}(\alpha)\boldsymbol{a}^{\mathrm{H}}(\alpha)}{\|\boldsymbol{a}(\alpha)\|^2}\frac{\partial \boldsymbol{a}(\alpha)}{\partial \alpha}\right]^{-1}$$

over α, must be carried out numerically.

Note that, somewhat unfortunately, eq. (10) rules out Swerling I model, because $\mathrm{EMCB}_{\mathrm{nc}}$ will be infinite.

3.2. Coherent processing case

When dealing with a coherent pulse burst it is not uncommon to apply coherent integration prior to actual detection and estimation. This reduces dimensionality of data to 1 and, at the same time, increases signal to noise ratio $n_P L$ times, where $0 < L < 1$ represents loss due to mismatch between assumed and actual target Doppler frequency. Using results from the previous subsection yields the following loss discounted FIM

$$[\mathbf{FIM}_c(\boldsymbol{\theta})^{-1}]_{1,1} = \frac{\sigma_v^2}{2n_P L B_T^2(\boldsymbol{w}_T, \alpha) F^2 r^2} \left[\left\| \frac{\partial \boldsymbol{a}(\alpha)}{\partial \alpha} \right\|^2 - \left(\frac{\partial \boldsymbol{a}(\alpha)}{\partial \alpha} \right)^{\mathrm{H}} \frac{\boldsymbol{a}(\alpha) \boldsymbol{a}^{\mathrm{H}}(\alpha)}{\|\boldsymbol{a}(\alpha)\|^2} \frac{\partial \boldsymbol{a}(\alpha)}{\partial \alpha} \right]^{-1} \tag{11}$$

which can be used to compute EMCB.

Remark: Observe that, perhaps counter-intuitively, (11) is larger than (9) by a factor of $1/L$. This stems from the fact that the processing method is not optimal. However, noncoherent processing may be much more sensitive to presence of clutter than coherent one. Hence, the latter still holds an advantage in clutter-limited scenarios.

4. Optimization

Direct optimization of (2)-(3) may be demanding in terms of computational complexity. Suppose however, that a set $\mathcal{W}$ of prespecified transmit distributions is available. Further, assume that $\mathcal{W}$ is a union of M disjoint sets $\mathcal{W}_m$, $m = 1, 2, \ldots, M$. Now suppose that for each $\boldsymbol{w}_T \in \mathcal{W}_m$ it holds that $Q(\boldsymbol{w}_T) = q_m$, i.e. $Q(\cdots)$ sets an order of preference, where all distributions in $\mathcal{W}_m$ are equally preferred with respect to each other. A reasonable example of such ordering is, e.g. to prespecify several choices of amplitude taper and rank available options according to sidelobe level.

Under such setup one can perform minimization of (2) subject to (3) with respect to n_P for each $\boldsymbol{w}_T \in \mathcal{W}$ separately. Then one can pick the optimal solution by comparing values of $f(\cdot)$ obtained during such independent optimizations.

Note that this search strategy can be parallelized in a straightforward way, if needed. Additionally an explicit formula the optimal value of n_P for a given $\boldsymbol{w}_T$ can be found, which reduces computational load. It takes the form

$$n_P = C_{\mathcal{N}_P} \left(\frac{\sigma_v^2}{2F^2 \Delta\alpha_{\max}^2} \mathrm{E}\left[r^{-2}\right] \mathrm{E}\left[G(\boldsymbol{w}_T, \alpha)\right] \right), \tag{12}$$

where $C_{\mathcal{N}_P}(x)$ denotes the operator of casting x to $\mathcal{N}_P$, i.e. choosing smallest admissible pulse trail length larger than x.

Two situations deserve special treatment. First, it may occur that the above procedure yields several array distributions with equal resulting $f(\cdot)$. Second, under adverse circumstances, all

choices of $\boldsymbol{w}_T$ may require pulse trails larger than largest element of $\mathcal{N}_P$ to satisfy accuracy constraint. In these situations, it is reasonable to prefer such a distribution $\boldsymbol{w}_T$ which yields the smallest mean-square estimation error.

5. Results of simulation

Our simulated radar system is fitted with a uniform linear array, consisting of 12 elements spaced at half wavelength. The array is tilted by 20 degrees upwards. We adopt sine of off-boresight angle as α, i.e.

$$\alpha = \sin[(\epsilon - \pi/9)]$$
$$\boldsymbol{a}(\alpha) = \begin{bmatrix} 1 & e^{j\pi\alpha} & e^{j2\pi\alpha} & \dots & e^{j11\pi\alpha} \end{bmatrix}^{\mathrm{T}},$$

where ϵ denotes elevation angle.

The simulation will feature a single Swerling III target with average RCS of $\sigma_{av} = 2.5$ m^2, traveling between $R_{\min} = 1000$ meters to $R_{\max} = 4000$ meters away from the radar at a height of 750 meters. Uncertainty of target's a'priori elevation angle varies with its distance form the radar. For simplicity we adopt the following formula for standard deviation of α

$$\sigma_\alpha = \frac{100}{R}$$

where R denotes target distance. The desired measurement accuracy is set to $\Delta\alpha_{\max} = 0.0035$.

The library $\mathcal{W}$ consists of three subsets $\mathcal{W}_1$, $\mathcal{W}_2$, $\mathcal{W}_3$. Each subset comprises of 23 beams, spaced uniformly between 2 and 48 degrees. The subsets differ from each other by amplitude taper. The subset $\mathcal{W}_1$ employs Chebyshev taper with -50 dB sidelobe level. The subset $\mathcal{W}_2$ also employs Chebyshev weights, this time with -30 dB sidelobes. Finally, $\mathcal{W}_3$ contains beams with uniform weighting.

Before moving ahead, let us make a brief comment on a particular choice of beams. The ultra low sidelobe beams are well suited for situations where a'priori angle uncertainty is rather high and SNR is not a problem. The other two options offer gradually increasing gain and power output to cope with weak targets at a long distance.

Generally, we prefer to use low-sidelobe beams, unless it results in excessive pulse trail length. To this end we adopt the following form of $Q(\boldsymbol{w}_T)$ in (2)

$$Q(\boldsymbol{w}_T) = \begin{cases} 0 & \text{for} & \boldsymbol{w}_T \in \mathcal{W}_1 \\ 8 & \text{for} & \boldsymbol{w}_T \in \mathcal{W}_2 \\ 32 & \text{for} & \boldsymbol{w}_T \in \mathcal{W}_3 \end{cases}$$

Finally, the set $\mathcal{N}_P$ consists of integers between 1 and 64, $\mathcal{N}_P = \{1, 2, \dots, 64\}$, and $F = 5 \cdot 10^7/R^2$.
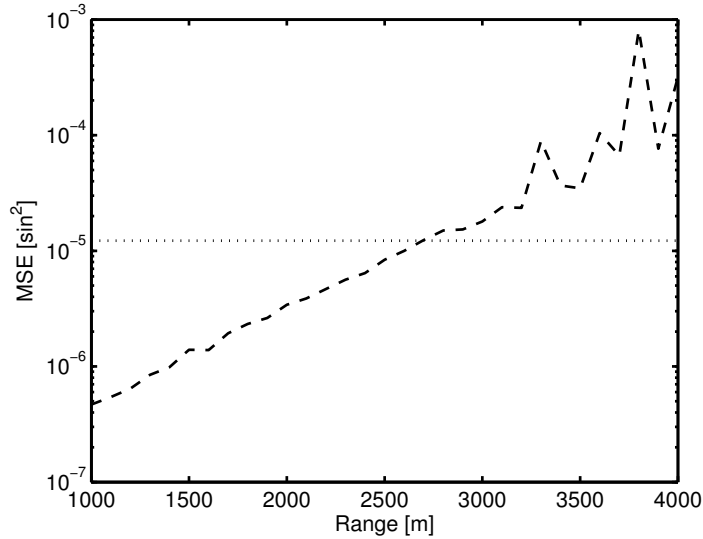
Figure 2: Comparison of mean squared angle estimation errors (dashed line) with their desired (fine-dotted line) values when fixed-parameter dwells are employed.

Fig. 2 shows mean squared elevation estimation errors when dwells with fixed parameters – $n_P = 32$ pulses and -50 dB weighting – are in use. Experimental means, computed by averaging 2000 realizations of $(\alpha, r, \phi_1, \ldots, \phi_{32}, \boldsymbol{v}_1, \ldots, \boldsymbol{v}_{32})$, are compared with desired mean square errors. It is obvious that performance goal is missed most of the time. For range smaller than 2500 m, the system is performing too well, i.e. one is spending excessive resources. Above 3000 m, the radar is not able to keep up with the goal and eventually we see signs of the threshold effect [6] – the growing fraction of large errors causes large spikes in the mean.

The situation is radically different when cognitive approach is used. Fig. 3 shows that the predicted and the actual MSE errors are always close to the assumed target. We can also see that dwells are scheduled in a very reasonable manner (Fig. 4): the system starts with low sidelobe beams and short pulse trails. It then increases n_P up to a certain point at which it makes more sense to sacrifice sidelobe level in order to save some time. This pattern is repeated again, when the system switches to uniform array weighting. After that, the only option left is to increase n_P, which is exactly what the system does.

6. Conclusions

The problem of optimizing time budget in tracking application was considered. A cognition-inspired solution, which balances dwell time and transmit beampatters sidelobe level, was proposed. Simulation results confirm that resulting radar performance stays close to desired values.

In this final paragraph of the paper we note that we are well aware that one could design a rule-based decision system with exhibiting a similar behavior. However, the important feature of cognitive approach is that the observed behavior is *emergent*, rather than *hard-coded*, feature of
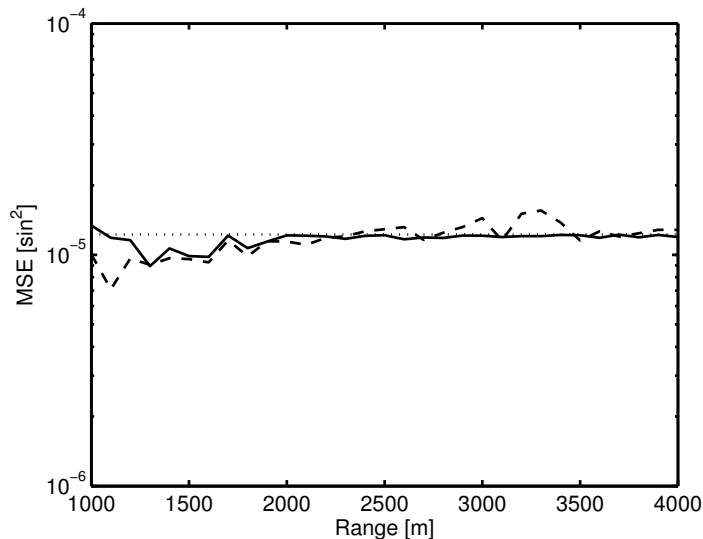
Figure 3: Comparison of mean squared angle estimation errors (dashed line) with their predicted (solid line) and desired (fine-dotted line) values when optimized dwells are employed.

the system. This marks a significant change of paradigm: rather than designing system behavior rules, the engineer is expected to specify goals and constraints while the cognitive system will 'simply do the rest'.

References

[1] D. K. Barton, "Radar System Analysis and Modeling", London: Artech House, 2005.

[2] K. L. Bell, C. J. Baker, G. E. Smith, J. T. Johnson, and M. Rangaswamy, "Cognitive radar framework for target detection and tracking", *IEEE Journal of Selected Topics in Signal Processing*, August 2015, vol. 9, no. 8, pp. 1427-1439.

[3] S. Haykin, "Cognitive Dynamic Systems: Perception-action Cycle, Radar and Radio", Cambidge: Cambridge University Press, 2012.

[4] J. Guerci, "Cognitive Radar: The Knowledge-aided Fully Adaptive Approach", London: Artech House, 2010.

[5] P. Swerling, "Radar probability of detection for some additional fluctuating target cases", *IEEE Transactions on Aerospace and Electronic Systems*, May 1997, vol. 33, no. 2, pp. 698-709, 1997.

[6] H. L. Van Trees, K. L. Bell, and Z. Tian, "Detection, Estimation, and Modulation Theory Part I", 2nd ed., New York: John Wiley & Sons, 2013.

[7] F. Gini and R. Reggiannini,"On the use of Cramer-Rao-like bounds in the presence of random nuisance parameters", *IEEE Transactions on Communications*, December 2000, vol. 48, no. 12, pp. 2120-2126.
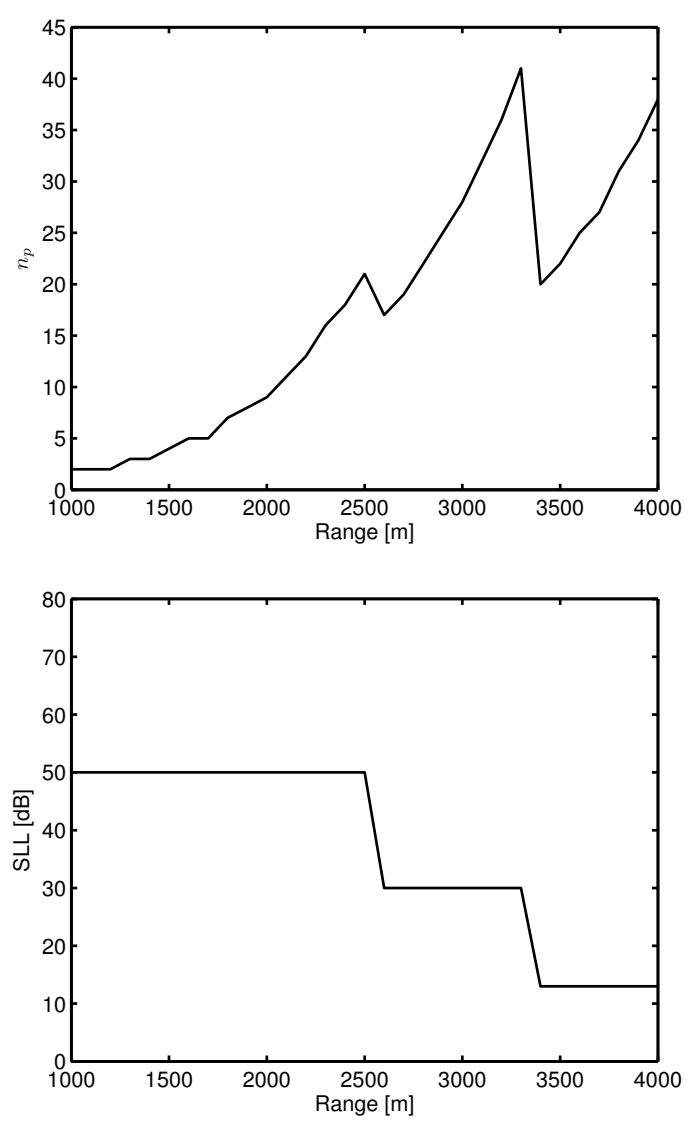
Figure 4: Number of pulses and transmit beam sidelobe level for dwells selected by the cognitive controller.